Effects of Position Quantization and Sampling Rate on Virtual-Wall Passivity

Jake J. Abbott and Allison M. Okamura, *Associate Member, IEEE*

Abstract—The "virtual wall" is *the* most common building block used in constructing haptic virtual environments. A virtual wall is typically based on a simple spring model, with unilateral constraints that allow the user to make and break contact with a surface. There are a number of factors (sample-and-hold, device dynamics, sensor quantization, etc.) that cause virtual walls to demonstrate active (nonpassive) behavior, destroying the illusion of reality. In this paper, we find an explicit upper bound on virtual wall stiffness that is a necessary and sufficient condition for virtual wall passivity. We consider a haptic display that can be modeled as a mass with Coulomb-plus-viscous friction, being acted upon by two external forces: an actuator and a human user. The system is equipped with only one sensor, an optical encoder measuring the position of the mass. We explicitly model the effects of position resolution, which has not been done in previous work. We make no assumptions about the human user, and we consider arbitrary constant sampling rates. The main result of our analysis is a necessary and sufficient condition for passivity that relies on the Coulomb friction in the haptic device, as well as the encoder resolution. We experimentally verify our results with a one-degree-of-freedom haptic display, and find that the system can display nonpassive behavior in two decoupled modes that are predicted by the necessary and sufficient condition. One mode represents instability, while the other mode results in active tactile sensations.

Index Terms—Coulomb friction, haptics, passivity, quantization, sampling, stability, virtual environments, virtual walls.

I. INTRODUCTION

MANY haptic virtual environments are created from fundamental building blocks known as "virtual walls." A virtual wall is typically an impedance surface accompanied by a unilateral constraint, where the impedance surface displays a force that is a function of the position (and its time derivatives) of the haptic device, and the unilateral constraint is a nonlinear switching condition that determines if the user *is* or *is not* in contact with the virtual wall. It is desirable to make virtual environments feel like real ones, but it is common for the user to feel an active behavior (often described as "vibration" or "rumble") that destroys the illusion of reality. This behavior is often associated with concept of passivity.

A passive system is incapable of generating a net amount of energy, and is defined by

$$\int_0^t f(\tau)v(\tau)\,d\tau + E(0) \geq 0 \quad \forall f(\cdot), v(\cdot) \quad \forall t \geq 0 \qquad (1)$$

where f and v are conjugate power variables that describe the energy flow into the system, and $E(0)$ is any energy stored in the system at time $t = 0$ [1]. All inanimate objects in the physical world are passive. When humans interact with a passive object in the real world, active behavior never results. This makes it easy to distinguish between real and virtual environments. Colgate *et al.* [2] give a description of how a virtual wall, implemented as a virtual spring, can become nonpassive, even though a physical spring is passive. Gillespie and Cutkosky [3] enumerate "energy leaks" through which the virtual wall can generate energy, such as zero-order hold (ZOH) and asynchronous switching times associated with a sampled unilateral constraint.

Creating a virtual wall that behaves passively has been an active area of research in the field of haptics. Colgate and Brown [4] catalog the limiting factors in stably generating stiffness with a haptic display. They cite sample-and-hold, device dynamics, position-sensor quantization, and velocity filtering as factors that limit the achievable stiffness of a virtual environment. They give a description of the errors incurred from obtaining a velocity estimate by differentiating a position measurement that was obtained with an encoder. Love and Book [5] use the Jury stability criterion to analyze contact instability. They assume the user can be modeled as an exogenous force input, thereby neglecting the dynamics of the user. Gillespie and Cutkosky [3] eliminate contact instability for a user modeled as a known, constant mass-spring-damper system. Colgate and Schenkel [6] present a simple condition on virtual-wall stiffness that is a function of the viscous friction in the system, as well as the sampling rate. Their result is a stiffness bound, below which the energy generated by "energy leaks" is dissipated by viscous friction in the haptic device, creating a system that appears passive to the user. Madill *et al.* [7] develop a nonlinear observer to estimate the position and velocity of the haptic device, as a way to deal with the effects of sensor quantization and Coulomb friction. However, their observer requires an accurate measurement of the force applied by the user. Goldfarb and Wang [8] implement a hysteresis coupled with a virtual spring as a way of ensuring virtual-wall passivity. They propose that one way to counter "energy leaks" is to simulate a dissipative system (rather than a lossless passive system). Adams and Hannaford [9] use a "virtual coupling" to ensure stable interaction with a virtual environment. This method essentially filters the impedance of
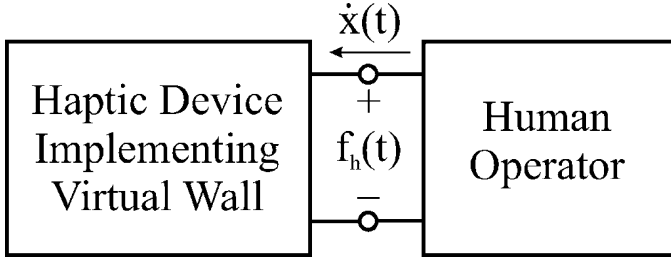
Fig. 1. Closed-loop system consisting of a human coupled with a virtual-wall system. Passivity of the individual blocks is sufficient for coupled stability.

the virtual environment, limiting the range of stiffness presented to the user. Hannaford and Ryu [10] introduce a Passivity Observer/Passivity Controller (PO/PC) that keeps track of the net energy generated by the virtual wall, and actively dissipates this excess energy. Ryu *et al.* [11] continue the PO/PC work by removing the previous assumption that the velocity of the haptic device remains constant between samples. In the most recent work by Ryu *et al.* [12], the PO/PC idea is extended to allow the dissipation of excess energy to take place over prolonged time periods, with the goal of reducing induced high-frequency vibration. Stramigioli *et al.* [13] use a port-Hamiltonian approach to explicitly keep track of energy as it moves through the system. Miller *et al.* [14] give conditions such that a quantifiable excess of passivity in a haptic device can be used to guarantee that a virtual environment will appear passive to the user. Finally, Mahvash and Hayward [15] use a dual-rate system that maintains passivity and fidelity when interacting with deformable virtual environments.

In creating various conditions for system stability or passivity, none of the previous work explicitly models quantization effects that occur from measuring position with an optical encoder, which is typical of haptic displays. In addition, much of the previous research mentioned uses some form of velocity measurement, without accounting for the fact that a quantized position measurement is typically used to compute a velocity estimate, introducing noise into the system (though adaptive velocity-estimation techniques can help to mitigate this effect [16]). Although it is almost never modeled, sensor quantization is widely acknowledged as a possible source of error, and explicit modeling of quantization effects is needed for improved accuracy of analytical results.

There are two motivations for designing virtual environments that appear passive at the driving point. The first, as previously discussed, is to eliminate the active tactile sensation that destroys the illusion of reality. Second, when a human interacts with a haptic device implementing a virtual wall, a closed loop is formed, as shown in Fig. 1. A sufficient condition for the coupled system to be stable is that each of the components in the system is passive [1], [17]. This relies on the assumption of human passivity for closed-loop stability [18], but experience interacting with the physical world says this is a safe assumption (that is, humans can behave passively when they choose to do so). Therefore, our second motivation for this research is to create systems with which humans can stably interact.

This paper is inspired by the philosophy of Colgate *et al.* [4], [6], in that we find a stiffness that is a simple function of the

system parameters and is guaranteed to result in a virtual wall that appears passive to the user. As in [6], the system is shown to be passive in that any "energy leaks" from the virtual wall are dissipated by the friction in the haptic device.

This work is different from previous work, though, due to a combination of important considerations. First, we explicitly consider sensor quantization. Second, we do not assume that the sampling rate of the computer is significantly faster than the bandwidth of the system, or that the ZOH elements can be modeled as linear time-invariant. Third, we make no assumptions about the human user. A typical assumption is that the sampling rate of the system is significantly faster than the human bandwidth, since at small time scales, human voluntary movement does not have time to enter into the analysis. Finally, we assume a more realistic friction model than only viscous friction. The biggest difference in our analysis from most literature in this field is that we make no assumptions about the sampling rate of the computer, or the resolution of the encoder, except that they are constant. We consider an arbitrarily slow computer, as well as an encoder with arbitrarily poor resolution. In addition, the human may implement the most malicious strategy possible in an attempt to extract energy from the wall (including generating trajectories with significant aliasing). In Section II, we present a detailed model of the system we consider.

Our main result is a simple necessary and sufficient condition on virtual-wall passivity that is a function of the friction present in the device, the sampling rate of the system, and the resolution of the position sensor. The result is given in Section III, and passivity is proven by showing that our nonlinear sampled-data system is always more dissipative than an ideal lossless system. The condition is validated experimentally in Section IV, and found to be a good predictor of system behavior. The experiments also yield insight into the modes of nonpassive behavior exhibited by these systems.

II. SYSTEM MODEL

The system we consider is given as Fig. 2. It is a one-degree-of-freedom (1-DOF) haptic device, modeled as a mass being acted upon by three forces—the force applied by the human user $f_h(t)$, the force applied by the actuator $f_a(t)$, and the force due to friction $f_f(t)$

$$f_h(t) - f_a(t) - f_f(t) = m\ddot{x}(t).$$

The human force $f_h(t)$ is defined as positive when it tends to move the haptic device forward into the virtual wall. The actuator force $f_a(t)$ and friction force $f_f(t)$ are both defined as positive when they tend to move the device out of the virtual wall. We adopt a Coulomb-plus-viscous-friction model [19]

$$f_f(t) = \begin{cases} f_c \mathrm{sgn}(\dot{x}(t)) + b\dot{x}(t), & \dot{x} \neq 0 \\ \min(f_c, |f_e(t)|)\mathrm{sgn}(f_e(t)), & \dot{x} = 0 \end{cases}$$

where f_c and b are the positive constant Coulomb and viscous-friction parameters of the haptic device, and $f_e(t) = f_h(t) - f_a(t)$ is the net external force on the mass. The quantized position signal is sampled with a constant sampling period of T. The quantized and sampled position measurement from the encoder is used as the measured penetration into the virtual wall, which
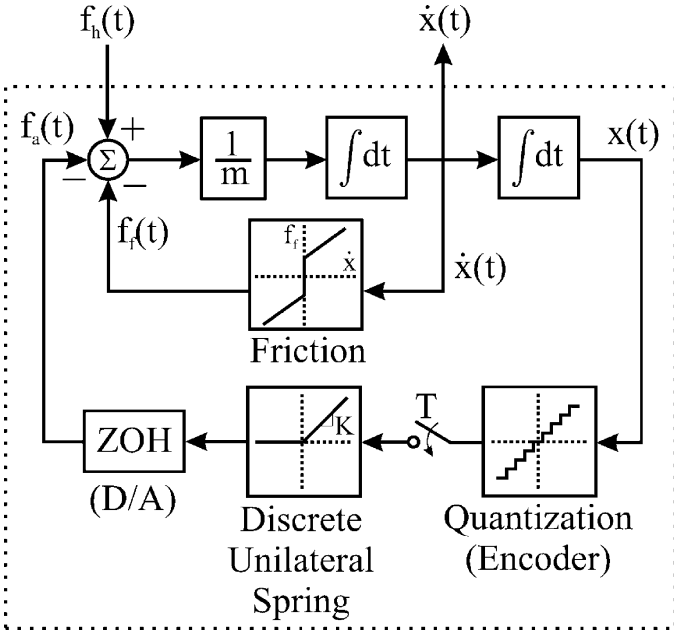
Fig. 2. Haptic device implementing a virtual wall. This is a sampled-data system, with device dynamics, sensor quantization, sampling, and ZOH considered explicitly.

is implemented, at sample k, as a simple discrete spring with a unilateral constraint

$$f_a(k) = \begin{cases} K x_{\mathrm{enc}}(k), & x_{\mathrm{enc}}(k) > 0 \\ 0, & x_{\mathrm{enc}}(k) \leq 0 \end{cases} \qquad (2)$$

where K is the stiffness of the virtual wall, and $x_{\mathrm{enc}}(k)$ is the measured position at sample k. The quantization is due to measuring position with an incremental optical encoder with a resolution of Δ. We focus on encoders due to their ubiquity in haptic devices, but the analysis to follow applies to any position quantization (such as discretizing an analog signal with an analog/digital (A/D) converter). The output of the discrete unilateral spring is held constant for the duration of the sampling period with a ZOH, resulting in a continuous-time staircase actuator force $f_a(t)$. It is clear that this simple virtual wall results in $f_a(t) \geq 0 \; \forall t$. We will exploit this property in our virtual-wall passivity analysis.

Sensor quantization is difficult to analyze accurately. It is a problem that exists independent of computer sampling, in that there is a fundamental loss of information, no matter how fast the sampling rate of the system. The mapping from the true position x to the measured position x_{enc} will exist somewhere between the two mappings shown in Fig. 3, for a given initialization, but where it lies is impossible to know. The quantization mapping will be time-invariant, though, until the system is reinitialized. We will assume, without loss of generality, that the solid line represents the quantization of the sensor. This assumption can be made because the true zero position of the device with respect to the encoder has no bearing on the problem. The only effect of this assumption will be to possibly change the value of $E(0)$ in (1), which does not affect the system passivity.
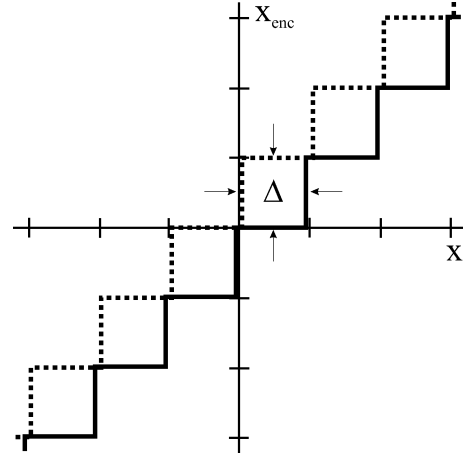

Fig. 3. Quantization mapping of encoder with resolution Δ falls somewhere between two extremes. Assume without loss of generality that the solid line represents quantization mapping.

III. VIRTUAL-WALL PASSIVITY

We now develop a virtual-wall passivity proof that uses a time-domain energy analysis. The proof makes use of a known passive (lossless) system as a reference system. If a haptic device implementing a virtual wall can be shown to be more dissipative than this lossless system in all cases, then the haptic device implementing the virtual wall is itself passive. The main result of the passivity proof is summarized as follows.

A haptic device implementing a virtual wall, as described in Section II, is guaranteed to be passive if and only if a simple condition is met

$$K \leq \min \left(\frac{2b}{T}, \frac{2f_c}{\Delta} \right). \qquad (3)$$

This condition on the maximum allowable virtual-wall stiffness involves two simple ratios—one between the viscous friction in the haptic device and the sampling period of the system, and one between the Coulomb friction in the haptic device and encoder resolution. We show later (in Section IV-C) that violating this condition physically results in systems that exhibit at least one of two types of nonpassive behavior: closed-loop instability and active-tactile sensations.

A. Approach

Consider an ideal mass-spring system, defined in compression when $x > 0$, and the only force acting on the system is that input by a human, f_h. This system is passive and lossless, since the total energy of the system at each instance in time (which includes kinetic energy of the mass and potential energy of the spring) is equal to the total work input by the human

$$W_h(t) = \int_0^t f_h(\tau) \dot{x}(\tau) \, d\tau. \qquad (4)$$

Now, consider the haptic device implementing the virtual wall shown in Fig. 2, with a mass equal to that in the ideal mass-spring system described above, and with a virtual spring constant equal to that of the spring described above. Previous work shows that a virtual wall (independent of the haptic device) is inherently nonpassive [2], [3]. In this section, we show that below some critical virtual-wall stiffness, the friction present in

a haptic device (which is not present in the ideal mass-spring system) will completely dissipate the energy generated by the discrete unilateral spring, making the system that contains both the virtual wall and the haptic device appear passive (or even dissipative) at the driving point.

We will conclude that a haptic device implementing a virtual wall is passive if and only if $W_h(t) \geq 0 \ \forall t \geq 0$. This will be accomplished by comparing the total energy (kinetic plus potential) in the haptic device implementing a virtual wall with that of the lossless ideal mass-spring system for all possible trajectories. The notion of kinetic energy translates easily between the physical mass-spring system and the haptic device; they are both simply $(1/2)m\dot{x}^2$. The notion of potential energy does not translate so trivially between an ideal spring and a virtual spring. This motivates Section III-B.1.

We now proceed by proving that (3) is the necessary and sufficient condition for passivity of the system of Section II. For sufficiency, we show that (3) guarantees that the system is incapable of generating any net energy. We then demonstrate the necessity of (3) by constructing counterexamples that result in net energy generation. For use in the remainder of this paper, we define the terms $x_0 = x(0), \dot{x}_0 = \dot{x}(0), x_T = x(T)$, and $\dot{x}_T = \dot{x}(T)$.

B. Sufficiency

We now consider four cases that span all possible scenarios encountered with the virtual wall: 1) starting inside the wall, and ending (one sample later) less deep or outside the wall; 2) starting inside the wall, and ending deeper inside; 3) starting outside the wall, and ending inside; and 4) starting and ending outside the wall. The result is a sufficient condition for virtual-wall passivity.

1) Moving Out of the Wall $(x_0 \geq 0, x_T \leq x_0)$: Consider an ideal mass-spring-damper system with a relaxed position at $x = 0$. The potential energy of this system at any given time is calculated as $(1/2)Kx^2$, even though this amount of energy could never practically be reclaimed from the system because of the viscous-friction losses associated with any movement. In this way, the potential energy is actually a supremum on the amount of latent energy in the system, and this upper bound is approached (but never reached) the more slowly the spring is released. We use this same notion to define the potential energy of the virtual wall. In this section, we determine what conditions must be met to use $(1/2)Kx^2$ as a measurement of potential energy of a virtual wall.

For any initial state condition $(x_0, \dot{x}_0)$, with $x_0 \geq 0$, consider the set of all possible trajectories, defined on the time interval $t \in [0, T]$, that move the device to some final state $(x_T, \dot{x}_T)$ with $x_T \leq x_0$. This includes both the case of leaving the wall, and the case of a final position that is less deep, but still within the wall. The energy balance for this scenario is

$$f_a(x_0 - x_T) + W_h = \frac{1}{2}m\left(\dot{x}_T^2 - \dot{x}_0^2\right) + W_f \qquad (5)$$

where W_h is the work input by the human [see (4)], W_f is a nonnegative quantity that includes all energy losses due to friction over the time interval, and f_a is the constant nonnegative

actuator force. Rearranging terms gives the work done on the human $W_1 = -W_h$ as

$$W_1 = f_a(x_0 - x_T) + \frac{1}{2}m\left(\dot{x}_0^2 - \dot{x}_T^2\right) - W_f. \qquad (6)$$

An ideal mass-spring system is conservative, so the energy extracted from it, for the same initial and final states considered above, is found simply as the sum of the losses in potential and kinetic energy

$$W_2 = \frac{1}{2}K\left(x_0^2 - x_T^2\right) + \frac{1}{2}m\left(\dot{x}_0^2 - \dot{x}_T^2\right). \qquad (7)$$

Consider the quantity $J = W_2 - W_1$, which represents the difference in the amount of energy extracted from the virtual wall and the ideal mass-spring for the same trajectory. If we can determine that J has a nonnegative lower bound, we can conclude that the potential energy of the virtual wall is no greater than the potential energy of the ideal mass-spring system, which is simply $(1/2)Kx^2$.

The problem of finding a lower bound on J, for a given set of initial and final state conditions, essentially becomes the problem of finding a lower bound on W_f in (6). It can be shown that the trajectory that minimizes friction losses is a monotonic trajectory with no stops of finite time (see the Appendix). This allows us to conclude that in the trajectory that minimizes J, the effects of Coulomb friction can be modeled as a constant retarding force f_c. This removes the nonlinear switching nature of Coulomb friction for the purposes of finding a lower bound on J. The performance index described above is then written as

$$J = \frac{1}{2}K\left(x_0^2 - x_T^2\right) + (f_a - f_c)(x_T - x_0) + \int_0^T b\dot{x}^2(t)dt. \qquad (8)$$

The problem of finding a lower bound on J simply becomes the problem of finding a lower bound on the viscous losses. We can use the Cauchy–Schwarz inequality [20] to find the lower bound on the viscous losses

$$\left(\int_0^T \dot{x}(t)\,dt\right)^2 \leq T \int_0^T \dot{x}^2(t)\,dt.$$

Using a result from the Appendix, we see that the left-hand side of the above equation is simply the square of the trajectory length. From this, we get an explicit lower bound on J

$$J \geq \frac{K}{2}(x_0^2 - x_T^2) + (f_a - f_c)(x_T - x_0) + \frac{b}{T}(x_T - x_0)^2. \qquad (9)$$

We now need to ensure that $J \geq 0$. The actuator force, defined in (2), can be rewritten as

$$f_a = K(x_0 - \delta) \qquad (10)$$

where $0 \leq \delta \leq \Delta$, but δ is otherwise unknown. The value of δ that minimizes the right-hand side of (9) is $\delta = 0$. Therefore, we can substitute $f_a = Kx_0$ into (9), and the worst-case J^* can be written as a function of initial and final states

$$J^* = \alpha(x_0 - x_T)^2 + f_c(x_0 - x_T) \qquad (11)$$

$$\alpha = \frac{b}{T} - \frac{K}{2}. \qquad (12)$$

It is interesting to note that J^* is only a function of the relative positions of the device, but not the velocities, at the endpoints.

This should not be surprising, since we can instantaneously input or extract finite amounts of kinetic energy (in the limit) through impulsive forces. Examination of the quadratic nature of (11) reveals that $J^* \geq 0$ whenever $x_0 - x_T \geq 0$, if $\alpha \geq 0$. This condition can be rewritten as a simple condition on the virtual-wall stiffness that may be implemented

$$K \leq \frac{2b}{T}. \tag{13}$$

If this condition is met, then the energy extracted from the virtual wall is always bounded from above by the energy extracted from an ideal mass-spring system with the same spring constant, mass, and initial conditions, and therefore, $(1/2)Kx^2$ can be used as a conservative estimate of potential energy in our virtual wall.

It should be noted that the equation used for W_2 (7) did not consider the unilateral constraint associated with an ideal mass-spring wall. Incorporating a unilateral constraint would only tend to increase W_2, and, in turn, increase J. Therefore, (11) is a conservative measure of the worst-case J when the user leaves the wall.

2) Moving Further Into the Wall $(x_0 \geq 0, x_T > x_0)$: In this section, we consider the case where the device starts within the wall $(x_0 \geq 0)$, and the user moves deeper into the wall $(x_T > x_0)$. Now that we are equipped with a simple representation of potential energy in the virtual wall, we want to guarantee that it is impossible to get free potential energy, which is the typical problem associated with implementing virtual walls [3]. In other words, we want to guarantee that any potential energy in the virtual wall that is gained during one sampling period is accompanied by *at least* as much prior work input by the human operator at the driving point.

For any initial condition $(x_0, \dot{x}_0)$, with $x_0 \geq 0$, consider the set of all possible trajectories, defined on the time interval $t \in [0, T]$, that move the device to some final state $(x_T, \dot{x}_T)$ deeper in the wall $(x_T > x_0)$. In this case, W_h, the work done by the human, is still found from the relationship in (5). An ideal mass-spring system is lossless, so the work done on it, for the same initial and final states considered above, is found simply as $W_3 = -W_2$ from (7). We now consider the quantity $J = W_h - W_3$, which represents the difference in the amount of work needed to compress the virtual wall and the ideal mass-spring along the same trajectory. A nonnegative value of J indicates that *at least* as much work is required to compress our virtual wall as it would have taken to compress an ideal mass-spring system along the same trajectory. If we can be assured that J has a nonnegative lower bound, we can conclude that it is impossible to get free potential energy from the virtual wall.

Again, the problem of finding a lower bound for J, for a given set of initial and final state conditions, becomes the problem of finding a lower bound for W_f. The performance index described above becomes

$$J = \frac{1}{2}K\left(x_0^2 - x_T^2\right) + (f_a + f_c)(x_T - x_0) + \int_0^T b\dot{x}_2^2(t)\,dt.$$

Note that the only difference between this equation and (8) is a sign change on f_c. The Cauchy–Schwarz inequality results in

$$J \geq \frac{K}{2}\left(x_0^2 - x_T^2\right) + (f_a + f_c)(x_T - x_0) + \frac{b}{T}(x_T - x_0)^2. \tag{14}$$

Again, note the sign change in f_c, and also in $x_T - x_0$, between this and the previous section. Using the actuator force of (10), the value of δ that minimizes J is $\delta = \Delta$. Therefore, we can substitute $f_a = K(x_0 - \Delta)$ into (14), and after some manipulation, the worst-case J^* can be written as a function of initial and final states

$$J^* = \alpha(x_0 - x_T)^2 + \beta(x_0 - x_T)$$
$$\beta = K\Delta - f_c \tag{15}$$

with α defined in (12). Analyzing the quadratic nature of (15) reveals that J^* has a minimum when $\alpha > 0$, and this minimum is nonnegative for $x_T > x_0$ when $\beta \leq 0$. This results in two simple conditions: that of (13), and

$$K \leq \frac{f_c}{\Delta}. \tag{16}$$

If these two conditions are met, we can be assured that the work required to compress the virtual wall is *at least* as large as the work required to compress a (passive) ideal mass-spring system with equivalent parameters.

The conditions of (13) and (16) form a sufficient condition for virtual-wall passivity, as was shown in [21], because we can construct a known passive device (the ideal mass-spring) that is less dissipative than the virtual wall in both compression and release. However, this result is overly conservative, because the virtual wall need not necessarily be more dissipative than the (lossless) ideal mass-spring in compression, *if* the virtual wall is significantly more dissipative than the ideal mass-spring during release. This is due to the virtual wall only being able to push, so that it can only generate energy during the release phase.

We find a less conservative sufficient condition if we replace (16) by

$$K \leq \frac{2f_c}{\Delta}. \tag{17}$$

This condition is equivalent to $\beta \leq f_c$. The sufficiency of (17), along with that of (13), is shown by considering Fig. 4. The left half of the plot shows J^* for compression [see (15)]. J^* can take on negative values, which would never be the case with (16). This worst-case J^* is lower bounded by the function $\beta(x_0 - x_T)$, which we will refer to as the linear-worst-case J^* for compression. It is clear that this function is always less than or equal to the worst-case J^*, therefore, it is *even worse* (in the sense of passivity). The right half of the plot shows the J^* for release [see (11)], which is lower bounded by the function $f_c(x_0 - x_T)$, which we call the linear-worst-case J^* for release. Again, this linear-worst-case is *even worse* than J^* in a passivity sense. Because the virtual wall can only push, and not pull, it is impossible to extract energy during a compression, and we know from consideration of the linear-worst-case functions for compression and release that any energy extracted during a release is guaranteed to be less than the amount required to compress the wall. In other words, it is alright if it takes less energy to compress the virtual wall than it would to compress an ideal mass-spring along the same trajectory, as long as the virtual wall is sufficiently dissipative during the release. Because of the linearity of the two linear-worst-case J^* functions, the conclusions hold for any combination of compressions and releases. We can,
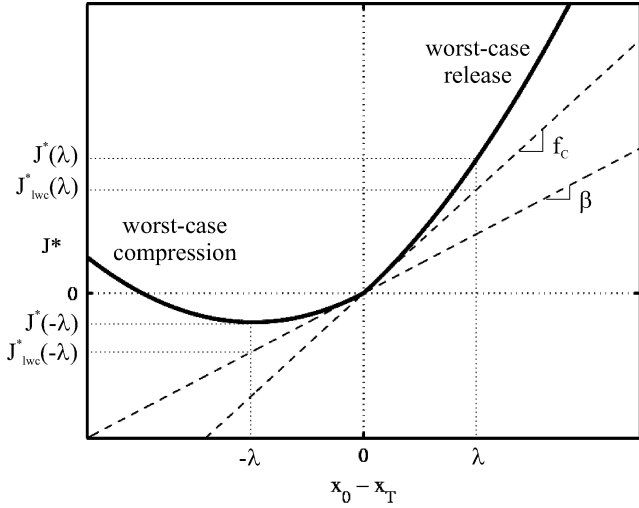
Fig. 4. Worst-case J^* for virtual-wall compression and release for a nominal system, with $\alpha > 0$ and $f_c \geq \beta$. Linear-worst-case lines are shown. $|J^*(\lambda)| \geq |J^*(-\lambda)|$ and $|J^*_{\text{lwc}}(\lambda)| \geq |J^*_{\text{lwc}}(-\lambda)|$ $\forall \lambda$.

Fig. 5. Worst-case J^* for virtual-wall compression and release for a nominal system, with $\alpha < 0$. Due to the quadratic nature of the curves, regardless of the sign of β, there will exist a closed kinematic trajectory that will result in net energy generation ($J^* < 0$ for compression and release).

therefore, conclude that it is impossible to extract a net amount of energy from the virtual wall, regardless of the trajectory.

3) Crossing Into the Wall $(x_0 < 0, x_T \geq 0)$: The third case considered is when the device begins outside the wall $(x_0 < 0)$ and ends inside the wall $(x_T \geq 0)$, corresponding to a wall crossing between samples. Any trajectory $x_c(t)$ that accomplishes this will have some time $T_c \in (0, T]$ when the device crosses the wall boundary, after which the device never leaves the wall (i.e., $x_c(t) \geq 0$ $\forall t \in [T_c, T]$). We can conclude from Section III-B.2 that any trajectory starting from the initial state $(x_0 = x_c(T_c), \dot{x}_0 = \dot{x}_c(T_c))$ and going to the final state $(x_T = x_c(T), \dot{x}_T = \dot{x}_c(T))$, which includes a trajectory that simply sits at the wall boundary for $0 \leq t \leq T_c$, would require *at least* as much work as the amount of potential energy gained. The trajectory we consider in this section requires this much work, *in addition to* the amount of work lost to friction just getting to the wall $(0 \leq t \leq T_c)$, with no gains in potential energy (because they end in the same location).

4) Staying Outside the Wall $(x_0 < 0, x_T < 0)$: This trivial final case is when the device starts outside the wall, and the user moves the device along a trajectory that also ends outside the wall. This case is obviously passive (dissipative if any movement occurs). Beginning outside the wall results in no actuator force, but friction still dissipates energy if any movement happens during the sampling period. Because the device will begin the next period outside the wall, the actuator will remain off, and therefore, no potential energy will be created.

C. Necessity

In the previous section, we showed that (13) and (17) together form a sufficient condition for the system of Section II to be passive. In this section, we show that this condition is also necessary for passivity. We accomplish this by constructing two simple examples to show that violating either (13) or (17) will result in a nonpassive system. The two examples also provide physical insight into the mode of nonpassive behavior that may be expected if either (13) or (17) is violated.
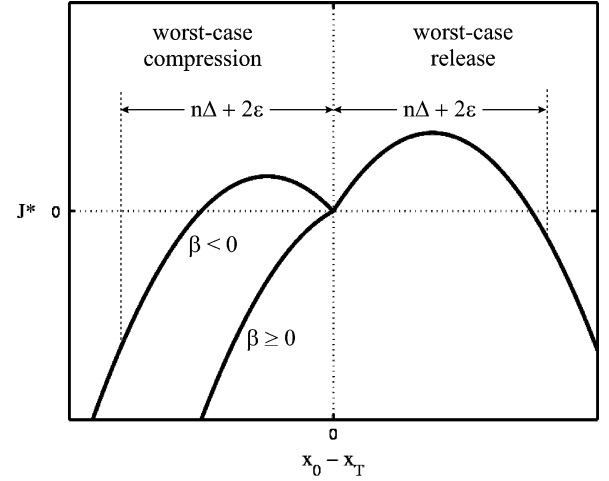
Consider a system with $K > (2b/T)$, which is equivalent to $\alpha < 0$. Fig. 5 shows the worst-case J^* values for compression and release of the virtual wall for a nominal system. Recall that the worst-case J^* for compression occurs when x_0 lies just on the negative side of an encoder pulse, and the worst-case J^* for release occurs when x_0 lies just on the positive side of an encoder pulse. From the figure, it is easy to see that due to the quadratic nature of J^*, and regardless of the value of β, there will exist some (possibly large) integer n, such that if the device is moved at a constant velocity in one sample period to a depth of $x_T = n\Delta + \epsilon$ (for some infinitesimal positive ϵ) from $x_0 = -\epsilon$, and then the device is withdrawn at a constant velocity back to $x = -\epsilon$ in the next sample period, the result is a net generation of energy. The net generation of energy is seen from the negative value of J^* in both compression and release of the wall. It is also easy to verify this generation of energy numerically. From this example of nonpassive behavior, it is evident that (13) is a necessary condition for passivity.

Next, consider a system with $K > (2f_c/\Delta)$. This is equivalent to $\beta > f_c$. The previous necessary condition exploited arbitrarily large movements; we will now exploit arbitrarily small movements (for visualization, imagine Fig. 4 when $\beta > f_c$). We again make use of some very small positive quantity $\epsilon < \Delta$. Consider a haptic device that starts from rest at a position $x_0 = \Delta - (\epsilon/2)$, and is then brought impulsively to a velocity $\dot{x} = (\epsilon/T)$. This velocity is held constant for one sample period, and then the device is brought to rest impulsively at a position $x_T = \Delta + (\epsilon/2)$. This movement requires a net input of energy from the human user of $W_{\text{in}} = (f_c + (b\epsilon/T))\epsilon$. At this point, the virtual wall switches on, with a value of $f_a = K\Delta$. Next, the velocity is brought impulsively to a velocity $\dot{x} = -(\epsilon/T)$, is held constant for one sampling period, and is then brought to rest impulsively at the original position $x = \Delta - (\epsilon/2)$. This movement extracts an amount of energy from the wall equal to $W_{\text{out}} = (K\Delta - f_c - (b\epsilon/T))\epsilon$. The question is whether $W_{\text{out}} > W_{\text{in}}$. This would indicate a net extraction of energy,

indicating a nonpassive wall. $W_{\text{out}} - W_{\text{in}} > 0$ can be rewritten, after some manipulation, as

$$\beta - f_c > \frac{2b\epsilon}{T}.$$

Because $\beta - f_c$ is some finite positive quantity, there will exist some (arbitrarily small) ϵ such that the above statement is true. Therefore, by repeating this simple motion, the user can extract an unlimited amount of energy from the virtual wall. From this example, it is evident that (17) is a necessary condition for passivity.

D. Discussion

The result of the previous sections is that the satisfaction of both (13) and (17) [written compactly as (3)] is necessary and sufficient for the system of Section II to be passive. The bound on virtual-wall stiffness in (3) indicates the importance of the relationship between viscous friction and sampling rate, and between Coulomb friction and encoder resolution. It also indicates a lack of coupling between the two sets of parameters. It seems intuitively obvious that increasing sampling rate, encoder resolution, and friction in the device would tend toward passivity, but it is not obvious that the relationships between these parameters would be so simple. A consequence of (3) is that at some point, increasing the system sampling rate leads to no additional ability to increase passive wall stiffness without first increasing encoder resolution. Likewise, at some point, increasing encoder resolution leads to no additional improvement without first increasing computer speeds. There is no reason to believe that, in general, the two bounds contained in (3) would even be of the same order of magnitude. It will likely be the case that the stiffness allowed (for guaranteed passivity) on a given nominal system will be sensitive to changes in *either* $(2b/T)$ *or* $(2f_c/\Delta)$, but not both.

The passivity proof presented shows that a haptic display implementing a virtual wall that satisfies (3) is guaranteed to satisfy (1) at every sample, but it is easy to show that this system actually satisfies (1) for all time (which is needed to truly claim passivity). To verify this, consider a system where (1) is violated at some instant between samples. A simple malicious-user strategy would be to bring the device instantly to a stop at that instant (extracting even more energy from the virtual wall), and then to hold the device still until the next sample, resulting in a violation of (1) at that sample. Thus, by contrapositive, a guarantee of passivity at the samples implies passivity for all time.

One of the most important contributions of this research is the knowledge that *no* system that can be modeled as in Section II can be passive if $f_c = 0$. Note that the part of our condition represented by (13) is very similar to the main result of [6] (which states that a virtual-wall system is passive if and only if $K < (2b/T)$ if no virtual damping is implemented). We have shown here that a system modeled as a mass-damper (i.e., only viscous friction) *is not* passive once quantization effects are considered.

The requirement that the friction in the haptic device can be modeled as Coulomb-plus-viscous friction may at first seem to be unrealistic (but surely less prohibitive than the common assumption of *only* viscous friction). But, increasing friction can only increase energy losses for a given kinematic trajectory.
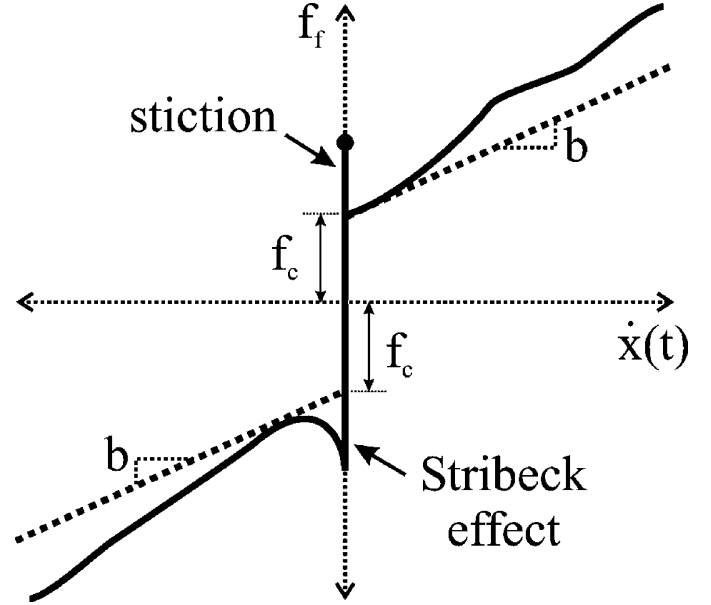

Fig. 6.   Friction containing "stiction" and nonlinear viscous friction, modeled as Coulomb-plus-viscous friction.

Therefore, if the magnitude of the friction of the device is always *at least* as large as the friction predicted by the Coulomb-plus-viscous model, then the device will still be guaranteed passive (i.e., sufficiency holds). Consider Fig. 6, where the friction in the device includes nonlinear viscosity, as well as "stiction" [19] (resulting from static friction that is larger than the dynamic friction). A device with this friction pattern could be modeled conservatively with the Coulomb-plus-viscous-friction model shown; the bound on stiffness from (3) will simply be more conservative than it would be otherwise. It is easy to verify that if the friction in the device can be modeled as "stiction" plus linear viscosity, then the necessity of the condition holds; the static friction can simply be overcome by impulsive input forces. Limitations in the friction model are discussed further in Section IV-C.

There is another factor that appears to contribute to (3) being conservative. The assumption that a human operator is capable of applying impulsive forces to the haptic device, leading to instantaneous changes in velocity, is obviously incorrect. Allowing these impulses appears to lead to a conservative model. Also, note that (3) says that the maximum allowable wall stiffness depends on every parameter in the model *except* the mass of the device. The mass of the device does come into play, though, in the conservative nature of the model. In this paper, impulsive forces can be thought of as a construct—a limiting behavior of real continuous bounded forces. For haptic devices with very low mass, the human operator will be able to create *nearly* instantaneous changes in velocity, while the inertia of devices with higher mass will prohibit rapid changes in velocity. Therefore, the model becomes more conservative as mass is increased. However, this conservative assumption of allowing impulsive forces at the input does not reflect on the *passivity* of the virtual wall, but rather on the *stability* of the closed-loop system containing the human operator. The passivity of the virtual wall is independent of the type of inputs it experiences—the system is either passive or it is not. That said, requiring a virtual wall to

be *passive* may be an overly conservative criterion if the actual desired result is *stable* human/wall interaction.

Another factor that led to the conservative nature of the proof is the use of the worst-case J^* in all of the analysis. The worst-case J^* must be considered to truly show passivity, but in practice, it only occurs under special circumstances. This assumption leads to a system that is actually dissipative (rather than just passive), meaning the system will lose any initial energy, making sustained oscillations impossible. It should be noted that the passivity proof of Section III only applies *directly* to the model of Section II. Real haptic devices may be thought of as fitting this model, with additional "modeling noise" present in the system. Because the virtual wall is dissipative, system passivity will be robust to some level of modeling error, provided the energy content of the modeling noise is relatively small. This robustness to modeling errors is verified experimentally in Section IV. Quantifying the amount of dissipativity in the virtual wall (i.e., the acceptable level of modeling errors) is left as an exercise for future work.

Possibly the largest drawback of the model used in this paper is the assumption that the actuator is an ideal force source that can apply any desired force instantaneously. This is a common assumption; in fact, none of the previous research discussed in Section I considers this problem, but in practice, an actuator will be limited by its own dynamics. Practically, the bandwidth of the actuator will likely be much higher than the bandwidth of the device being controlled. Current amplifiers can also be used in place of traditional voltage amplifiers to mitigate the effects of actuator dynamics. In addition, the digital/analog (D/A) card communicating desired forces to the actuator will have limited resolution. The implicit assumption is that the resolution of the D/A will be relatively small (we also do not consider resolution of floating-point numbers in the computer, which will have even better resolution). Also, actuator saturation was not considered in our analysis, and this could affect the necessity of (3). Our methodology is very different from that used in previous work, and could be used to address actuator limitations and D/A resolution. The assumptions surrounding the actuator are addressed in more detail in Section IV-B. An improved actuator model may need to be considered in future work.

Finally, it would be very desirable to include a virtual damping term, in an analysis similar to that considered here. It has been shown that adding virtual damping makes a virtual wall *feel* stiffer to the user, without an actual increase in stiffness. The problems inherent with measuring velocity from an encoder signal make the inclusion of virtual damping in a *guaranteed* passive virtual wall difficult. Salcudean and Vlaar [22] show that implementing a "braking pulse" when entering a virtual wall is an alternative way of improving the perceived stiffness of the wall. This approach may fit in better with the methods presented here, as may other forms of "open-loop" velocity feedback [23]. Inclusion of some form of active damping is an important problem for future work.

IV. EXPERIMENTAL VERIFICATION

We now verify the necessary and sufficient condition for virtual-wall passivity using a simple 1-DOF haptic display known
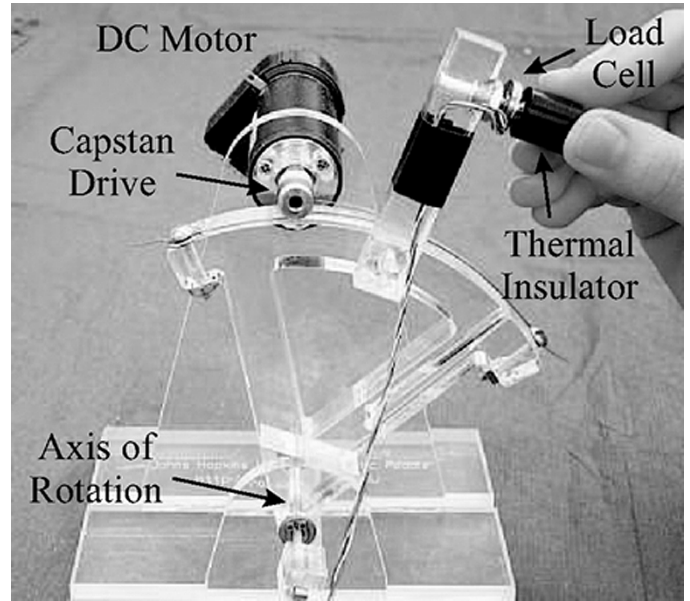

Fig. 7. Modified Haptic Paddle.

as the Haptic Paddle [24]. For a general nonlinear system, it is impossible to prove passivity experimentally (because it would require us to move the device along all possible trajectories), but it *is* possible to demonstrate nonpassive behavior. In this section, we attempt to generate nonpassive behavior, and the resulting behavior supports (3) as a useful measure of passivity in real systems.

A. Experimental Haptic Device

The Haptic Paddle considered here has been modified with a Maxon DC motor (model 118754) with a 500-counts-per-turn Hewlett-Packard encoder. We have also added an Entran ± 10-N load cell (model ELFS-T3E-10N) to measure the applied user force. A Delrin cap was added to thermally insulate the load cell. The modified Haptic Paddle is shown in Fig. 7. The device properties are typical of haptic displays (backdrivable, low friction, low inertia, low backlash). We use the PCI-DAS6402 data-acquisition card from Measurement Computing Inc. to output voltages to the motor amplifier and to input voltages from the load cell. The 16-b D/A is configured for ± 10 V, and the 16-b A/D is configured for ± 1.25 V. The output of the D/A is passed through a current amplifier that gives a current through the motor that is proportional to the D/A voltage ($i = 0.33v$); the current amplifier is built around a National Semiconductor LM675 power op-amp. This gives us direct control of applied torque on the motor. The resulting system has a force felt at the driving point that is proportional to the output voltage (1.65 N/V) statically. The signal from the load cell is passed through an instrumentation amplifier (Burr-Brown INA103) with a gain of five before it is read by the A/D. We use the PCI-Quad04, also from Measurement Computing, to interface with the encoder. The virtual-wall control loop is implemented at a maximum rate of 1000 Hz ($T = 0.001$ s), and the highest position resolution at the driving point is $\Delta = 2.24 \times 10^{-5}$ m.

B. Device Model

We begin by modeling our Haptic Paddle as in Section II. The Haptic Paddle is a rotational system, but we can find the equivalent linear system felt at the load cell as it moves along an arc. At every instant in time, when the device is in motion, the unactuated system should follow

$$m\ddot{x}(t) = f_h(t) - b\dot{x}(t) - f_c \text{sgn}(\dot{x}(t)).$$

By sampling the system at many instances, we may construct the matrix equation

$$[\ddot{\mathbf{x}} \quad \dot{\mathbf{x}} \quad \text{sgn}(\dot{\mathbf{x}})][m \quad b \quad f_c]^T = \mathbf{f_h}.$$

This system can be written compactly as $\mathbf{Ap} = \mathbf{f_h}$, with data matrix $\mathbf{A}$ and parameter vector $\mathbf{p}$. The best estimate of the parameter vector, in a least-squares (LS) sense, is found as $\mathbf{p} = \mathbf{A}^\dagger \mathbf{f_h}$, which uses the pseudoinverse of $\mathbf{A}$ based on singular value decomposition [25] (also known as the Moore–Penrose generalized inverse [26]).

To construct the $\mathbf{A}$ matrix, we "randomly" forced the system by hand while grasping the thermal insulator. Four runs of data were taken, with the load cell unloaded and zeroed between each run. This was done to mitigate the effects of drift in the force measurement. Position and force data were recorded at each sample, and the position data was then used to construct the velocity and acceleration data. Because of the staircase discontinuous position measurement, the position data was smoothed offline using a multiple-pass, three-point, moving-average filter [27] before differentiation. The velocity data was also smoothed before differentiation. The data sets were finally stacked to create the $\mathbf{A}$ matrix and the $\mathbf{f_h}$ vector, with a total of nearly 100 000 samples. Note that the force $f_c \text{sgn}(\dot{x}(t))$ is only valid when $\dot{x}(t) \neq 0$. Because we never allowed the device to stay at rest while taking data, the samples occurring at zero velocity are few, and should have little effect on the resulting LS solution.

The resulting best-fit parameters are $m = 0.036$ kg, $b = 0.15$ Ns/m, and $f_c = 0.12$ N, with $r^2 = 0.95$, indicating a very good fit of the model [28]. The distribution of the data indicated that the r^2 metric is appropriate as a measure of how well the model fits the data. Note that a perfect fit ($r^2 = 1$) is essentially unattainable because of the noisy force and position measurements. Using these parameter values, we compute $(2b/T) = 300$ N/m and $(2f_c/\Delta) = 10\,700$ N/m. Therefore, for our haptic paddle, the stiffest passive virtual wall that can be implemented is $K = 300$ N/m. For our system, the term based on viscous friction and sampling rate dominates over the term based on Coulomb friction and encoder resolution. Practically, we must increase the sampling rate of our system for any additional gains in wall stiffness.

It is interesting to note that if we were to attempt to model our system as mass-damper system, as in [6], the resulting LS fit would give $m = 0.036$ kg and $b = 0.41$ Ns/m, which would indicate that $K = (2b/T) = 820$ N/m would be passive. But this stiffness is nearly three times too large, indicating that fitting a mass-damper model to our system could be detrimental in this setting. An r^2 value of 0.92 verifies a poorer fit for the mass-damper model.

In Section III-D, we discussed the assumptions surrounding the ideal actuator in our model. That is, that the quantization in the actuator signal is small, relative to the quantization effects of the position measurement, and that the bandwidth of the actuator is much faster than the sampling rate of the computer. It only makes sense to compare the force (D/A) resolution with the position resolution for a given wall stiffness, so we compute the force resolution for the virtual wall with a stiffness of 300 N/m, using the information provided in Section IV-A. We find that the force resolution is 13 times finer than the position resolution for this stiffness—an order of magnitude better. For stiffer virtual walls, the force resolution will only improve relative to the position resolution (since a single step in quantized position corresponds to many steps in quantized force).

Next, we consider the rise time of the power amplifier. The bandwidth of the op-amp itself is many orders of magnitude faster than the other time constants in the system, so it will not be considered explicitly. For our system, the factors limiting the actuator rise time are the inductance in the motor, and the saturation limits of the amplifier. Ideally, the inductance in the motor would have no effect when using a current amplifier, but this would require voltages that are well beyond the ± 12-V output limit of the amplifier. Therefore, when a constant current is commanded from the amplifier, the inductance in the motor forces the amplifier to saturate to its maximum achievable voltage, and the maximum rate of change in current is given by

$$\left(\frac{di}{dt}\right)_{\max} = \frac{v_{\max}}{L}.$$

For our motor, the inductance is $L = 0.55$ mH, resulting in a maximum rate of change in current of 21 800 A/s. For the longest rise time possible, we consider an instantaneous change in current command from 0 to 3.3 A, the largest current we can command to our motor. For this scenario, the rise time would be 0.15 ms, which is 15% of the sampling period. In any practical application, we will not experience this worst-case scenario, and the rise time of the amplifier will be *much* faster, making the amplifier speed an order of magnitude faster than the sampling rate of the system. Increasing the supply voltage to the op-amp would also help to mitigate this effect. With the above considerations, we conclude that the modeling assumption of an ideal actuator is safe, with respect to the other modeled elements in the system.

C. Experimental Results

In this section, we show that the passivity condition given in (3) is a good predictor of passive behavior in real systems. Specifically, violation of (13) is shown to result in unstable closed-loop systems, while violation of (17) is shown to generate active-tactile sensations.

We begin by exploring the physical implications of (13). Fig. 8 shows interactions with a virtual wall with stiffness $K = 300$ N/m, which was predicted to be the stiffest possible passive wall for our system. The figure shows a "typical" touch, where the user holds the device at the load cell, moves at a moderate speed toward the wall, and then attempts to press against the wall with a constant force. The figure also shows a "malicious" touch, where the user learned how best to make
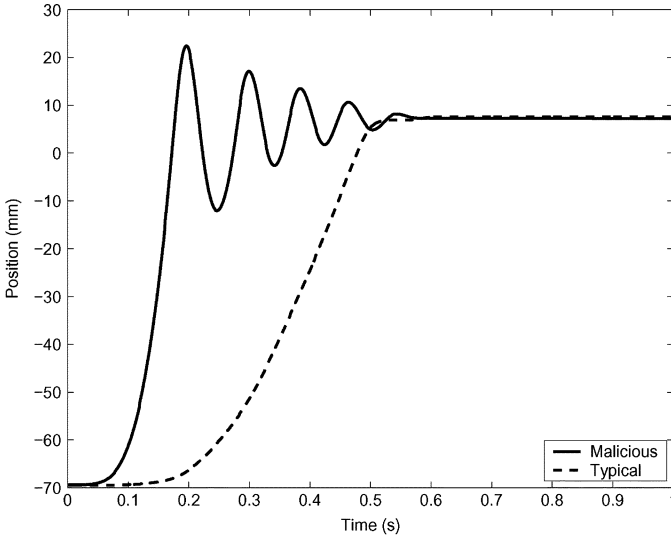
Fig. 8. Experimental data resulting from typical and malicious touch with $K = 300$ N/m. Positive values correspond to virtual-wall penetration. This plot supports passivity.
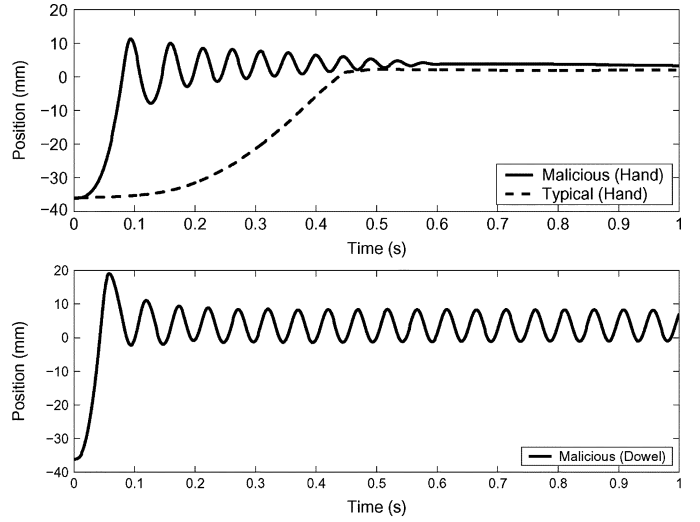

Fig. 9. Experimental data resulting from typical and malicious touch with $K = 770$ N/m, and from a malicious touch with a wooden dowel for the same stiffness. Positive values correspond to virtual-wall penetration. The human finger can not exploit the active behavior at this stiffness.

the device vibrate against the wall. This was done by pressing much lower on the device, moving very quickly toward the wall, and matching the resonance frequency of the finger with that of the wall (note that the user was attempting to touch the wall with a constant force—the oscillations seen are not the result of voluntary movement). At this wall stiffness, the user was unable to create sustained vibrations. This is evidence supporting the claim of passivity. Note that although sustained vibrations were not generated, the wall is not over damped at this stiffness; it took multiple bounces before the initial kinetic energy was dissipated. This is evidence that the condition on virtual-wall passivity is not so overly conservative as to be unuseful.

Fig. 9 shows interactions with a virtual wall with $K = 770$ N/m. The user was unable to create sustained oscillations by using the "malicious" strategy discussed above, but the response is more underdamped than that seen in Fig. 8. It appears, though, that more typical interactions with this wall are well behaved (as well behaved as the "typical" touch seen in Fig. 8). But when the user interacts with the haptic device through a wooden dowel, the figure clearly displays active behavior. This active behavior shows that this wall *is not* passive. The wooden dowel embodies an impedance that the human finger is unable to achieve. This stiffness is over twice as large as that predicted for passivity, but it is conceivable (even likely) that interacting with the virtual wall through other "tools" would push the difference between the predicted and experimentally validated passive stiffness values even lower. In Section IV-B, we found that modeling our device as a mass-damper, and then applying the passivity condition of [6], would result in a predicted passive stiffness of $K = 820$ N/m. It is clear than the upper bound on passive virtual-wall stiffness for our system is below this value.

It is unlikely that any real interaction would ever create the conditions needed to generate energy (see Section III-C) at stiffness just slightly greater than the upper bound for passivity, but Fig. 8 shows that system passivity may be a good predictor of possible undesirable behavior.

Next, we consider the physical implications of (17). For our system, we found that $(2b/T)$ was the limiting quantity, so our sampling rate must be increased to implement stiffer passive walls. But this may not be the case for other systems. To explore this notion, we now artificially lower the resolution of our encoder by a factor of 100, resulting in a maximum passive stiffness of $(2f_c/\Delta) = 107$ N/m.

The second necessary condition of Section III-C provides insight into the mode that the system will exhibit nonpassivity. That necessary condition exploited very small movements that straddled an encoder pulse. In fact, we find that this is exactly how the system becomes nonpassive, and the resulting active feeling destroys the illusion of reality during interaction with the virtual wall. Fig. 10 shows a user interacting maliciously with three different virtual walls. In this case, a malicious interaction (that which most exploits nonpassive behavior) is simply touching the wall very softly. For stiffness values of $K = 240$ N/m and $K = 120$ N/m, the user feels a buzzing sensation, an active behavior than no real (passive) environment would exhibit. For a stiffness of $K = 80$ N/m, the user was unable to create this phenomenon; the variance seen for this stiffness is simply due to the imprecision in human force control. In general, the energy content of the active behavior increases with increasing stiffness, as seen in the first two plots. Fig. 11 shows experimental data of a malicious touch for a stiffness of $K = 90$ N/m. For our system, this appears to be near the boundary of passive behavior. The user had to consciously work to exploit the nonpassivity, as is evident in the plot. The corresponding position data confirms that the active behavior felt by the user is, in fact, due to straddling an encoder pulse.

The stiffness predicted by (3) is a good predictor of the limits on passivity due to quantization, but it slightly overestimated the actual boundary of passivity found experimentally. This is likely due to inaccuracies in our friction model. More comprehensive friction models than the Coulomb-plus-viscous-friction model, such as that in [29], include hysteresis loops, due largely to potential energy stored at the asperity level. This can make
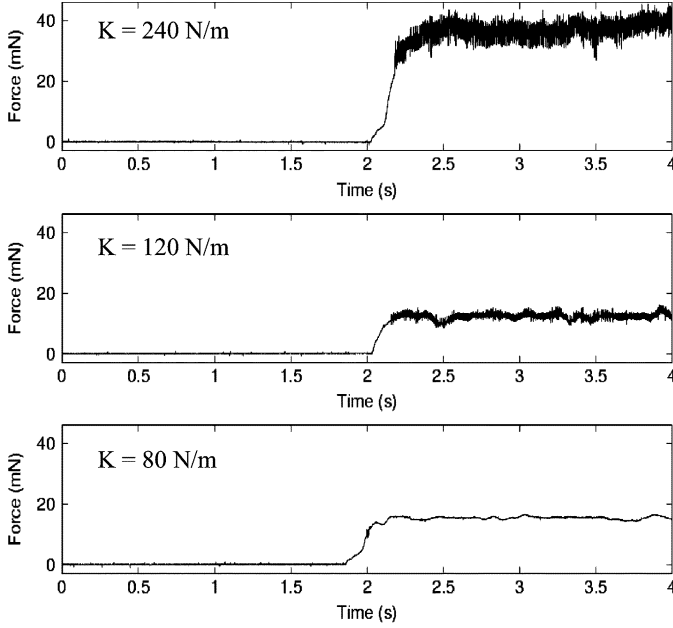
Fig. 10.   Experimental force data, measured by the load cell, resulting from malicious touch with three virtual-wall stiffness values. The user touched the virtual wall very softly at approximately the 2-s mark. This virtual wall behaves passively only for $K = 80$ N/m.
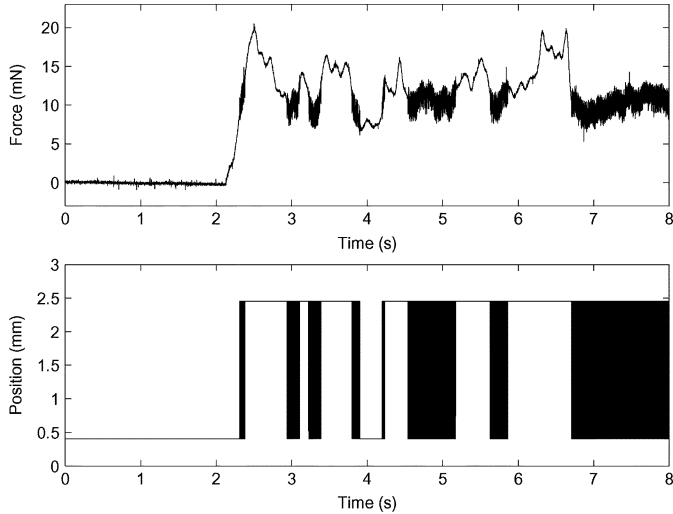

Fig. 11.   Experimental force data, measured by the load cell, resulting from malicious touch with $K = 90$ N/m. The user touched the virtual wall very softly at approximately the 2-s mark. This stiffness value appears to be the "boundary" of passivity for our system—it is difficult for the user to generate nonpassive behavior. Position data confirms that nonpassive behavior occurs when straddling an encoder pulse.

"friction" appear to actually generate small amounts of energy when the device changes direction. The small periodic movements used to exploit nonpassivity due to quantization may also be exploiting the inaccuracies in the model, making (3) slightly overpredict the achievable passive stiffness. It is also possible that obtaining an estimate of f_c through a method other than the pseudoinverse method would result in a more accurate model.

It is interesting to note that the two modes in which the system can become nonpassive experimentally appear to be largely decoupled. For the system with reduced encoder resolution, we repeated the experiment shown in Fig. 9, and we observed almost

no change from the previous experiment (approximately 5%), even with a substantial difference in encoder resolution. This experiment was accompanied, though, by a high-frequency vibration, due to quantization, that was not felt in the experiment of Fig. 9. We performed an additional experiment where, for the system with reduced encoder resolution, we slowed down the sampling rate to $T = 0.003$ s, and repeated the experiment of Fig. 11. We observed a very small change in the boundary of passive behavior (approximately 10%), but the active behavior *felt* different—the vibrations were of lower frequency and larger magnitude.

The result of this experimental verification is that the passivity condition given in (3) is a good predictor of the limit in virtual-wall stiffness for desirable behavior in real systems. In addition, the two modes in which the system can behave nonpassively correspond directly to the two motivations for passivity research that were introduced in Section I: creating stable coupled systems, and creating virtual environments that feel realistic. Physically, violation of (13) corresponds to nonpassivity in a closed-loop-stability sense, while violation of (17) corresponds to nonpassivity in an active-tactile sense.

V. CONCLUSION

We have given a simple explicit upper bound on virtual-wall stiffness that is necessary and sufficient for virtual-wall passivity. A passive user, interacting with such a wall, is incapable of generating sustained vibration. We considered a haptic display that can be modeled as an actuated mass with Coulomb-plus-viscous friction, but the condition also applies directly to a larger class of friction models that consider "stiction." In addition, the sufficiency of the condition applies to an even larger class of friction models that consider nonlinear viscous friction. We explicitly considered the effects of a quantized position measurement. We also removed common assumptions about the human user and the sampling rate of the system. The results presented here show a decoupling of the effects of sampling rate and encoder resolution, and give useful design criteria for generating stiffer passive virtual walls. A simple experiment provided evidence that the results presented are applicable to real systems, and lead to a significant new (quantifiable) understanding of nonpassive behavior in haptic devices implementing virtual walls.

APPENDIX

We present two intuitive energy concepts used in the analysis in the paper. These concepts increase our knowledge about trajectories that minimize friction losses over one sampling period. The result is that, for the trajectory (with fixed starting and ending states) that minimizes energy losses due to friction, the component of friction due to Coulomb friction will be constant in magnitude and direction.

A. Monotonic Trajectories

We first show that when moving the unactuated haptic device of Section II from any given initial state $(x(0), \dot{x}(0))$ consisting of position and velocity to any given final state $(x(T), \dot{x}(T))$, the trajectory $x(t)$ that minimizes energy losses due to friction

is monotonic. We assume without loss of generality that $x(T) \geq x(0)$, and the monotonic trajectory is, therefore, nondecreasing, i.e., $\dot{x}(t) \geq 0 \ \forall t \in [0, T]$.

The energy losses for the trajectory $x(t)$ due to Coulomb friction are found by

$$W_{cf} = \int_0^T f_c |\dot{x}(t)| \, dt.$$

A lower bound on the Coulomb losses is found with

$$f_c \int_0^T |\dot{x}(t)| \, dt \geq f_c \left| \int_0^T \dot{x}(t) \, dt \right| \qquad (18)$$

where equality is reached only when $x(t)$ is monotonic [20].

The energy losses due to viscous friction are also minimized when $x(t)$ is nondecreasing. The argument to prove this is simple: given any continuous but otherwise arbitrarily complicated trajectory $x_1(t)$, in which $\exists t \in [0, T]$ such that $\dot{x}_1(t) < 0$, we can easily construct a nondecreasing trajectory $x_2(t)$ with smaller viscous friction losses than those due to $x_1(t)$. We will construct $x_2(t)$ by parameterizing $x_1(t)$ along the trajectory

$$x_2(t) = \frac{x_1(T) - x_1(0)}{\int_0^T |\dot{x}_1(s)| \, ds} \int_0^t |\dot{x}_1(s)| \, ds. \qquad (19)$$

The losses due to viscous friction are found by

$$W_{vfi} = \int_0^T b \dot{x}_i^2(t) \, dt. \qquad (20)$$

To show that the viscous friction losses in $x_2(t)$ are smaller than those in $x_1(t)$, it follows from (20) that it is sufficient to show that $\dot{x}_2^2(t) < \dot{x}_1^2(t) \ \forall t$. Differentiating (19) and squaring gives

$$\dot{x}_2^2(t) = \left(\frac{x_1(T) - x_1(0)}{\int_0^T |\dot{x}_1(s)| \, ds} \right)^2 \dot{x}_1^2(t)$$

resulting in

$$\frac{W_{vf2}}{W_{vf1}} < 1.$$

It should be noted that creating $x_2(t)$ as a parameterization of $x_1(t)$ in this way results in a discontinuity in $\dot{x}_2(t)$ at the endpoints. That is to say, $\dot{x}_2(0) \neq \dot{x}_2(0^+)$ and $\dot{x}_2(T) \neq \dot{x}_2(T^-)$. This is not a problem if impulsive forces are considered, which create this type of discontinuity in velocity. The impulses needed to create $x_2(t)$ occur over infinitesimal distances, so they result in no energy losses due to either Coulomb or viscous friction. These impulses represent the limiting behavior of bounded continuous forces.

B. No Resting

The previous result shows that when moving the unactuated haptic display from any initial state to any final state, the trajectory that minimizes energy losses due to friction is monotonic. This essentially means the mass may not "turn around," but it could potentially stop for some duration of time. In this section, we prove that the trajectory that minimizes energy losses due to friction is one that contains no finite periods of zero velocity (i.e., any stops that the trajectory may contain are of infinitesimal duration). We show this by taking any arbitrary trajectory
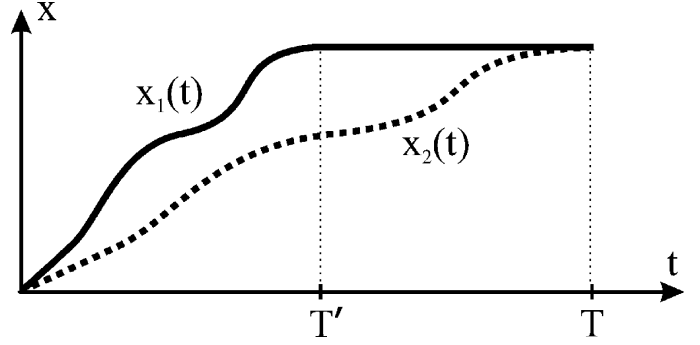

Fig. 12. Dynamic portion of $x_1(t)$ is "stretched" in time to create $x_2(t)$, containing no resting region.

that contains periods of rest, and constructing a trajectory with no resting that results in less frictional losses than the original.

Consider Fig. 12. The trajectory $x_1(t)$ has zero velocity for time $t = T'$ to $t = T$, and is monotonic but otherwise arbitrary before $t = T'$. No Coulomb or viscous frictional losses are experienced during the rest phase, so the two losses can be expressed, respectively, as

$$W_{cf1} = \int_0^{T'} f_c |\dot{x}_1(t)| \, dt$$

$$W_{vf1} = \int_0^{T'} b \dot{x}_1^2(t) \, dt.$$

Now construct the trajectory $x_2(t)$ by "stretching" the dynamic portion of $x_1(t)$ in time

$$x_2(t) = x_1 \left(\frac{T'}{T} t \right). \qquad (21)$$

Because both trajectories have the same length (given by $|x_1(T') - x_1(0)|$), their energy losses due to Coulomb friction are equal ($W_{cf2} = W_{cf1}$). The viscous losses in $x_2(t)$ are found by

$$W_{vf2} = \int_0^T b \left(\frac{d}{dt} x_2(t) \right)^2 dt. \qquad (22)$$

This is simply a restatement of (20). We will consider the change of variables

$$s = \frac{T'}{T} t$$

which, when combined with (21) and (22), results in

$$W_{vf2} = \frac{T'}{T} \int_0^{T'} b \left(\frac{d}{ds} x_1(s) \right)^2 ds. \qquad (23)$$

Therefore, we can conclude that the viscous losses in $x_2(t)$ are less than those of $x_1(t)$, since

$$\frac{W_{vf2}}{W_{vf1}} = \frac{T'}{T} < 1. \qquad (24)$$

Now that the total friction losses in $x_2(t)$ are found to be less than those in $x_1(t)$, we can apply this result to a monotonic, but otherwise arbitrary, trajectory with more than one period of rest. Simply break the trajectory into segments that contain only one period of rest, and then "stretch" each segment in time as

described above. We also note that including the resting region of $x_1(t)$ at the beginning rather than end would not change the result.

ACKNOWLEDGMENT

REFERENCES

[1] C. A. Desoer and M. Vidyasagar, *Feedback Systems: Input-Output Properties*. New York: Academic, 1975.
[2] J. E. Colgate, P. E. Grafing, M. C. Stanley, and G. Schenkel, "Implementation of stiff virtual walls in force-reflecting interfaces," in *Proc. IEEE Annu. Virtual Reality Int. Symp.*, 1993, pp. 202–208.
[3] R. B. Gillespie and M. R. Cutkosky, "Stable user-specific haptic rendering of the virtual wall," *Proc. ASME Dyn. Syst. Control Div.*, vol. 58, pp. 397–406, 1996.
[4] J. E. Colgate and J. M. Brown, "Factors affecting the z-width of a haptic display," in *Proc. IEEE Int. Conf. Robot. Autom.*, 1994, pp. 3205–3210.
[5] L. Love and W. Book, "Contact stability analysis of virtual walls," *Proc. ASME Dyn. Syst. Control Div.*, vol. 57, no. 2, pp. 689–694, 1995.
[6] J. E. Colgate and G. G. Schenkel, "Passivity of a class of sampled-data systems: Application to haptic interfaces," *J. Robot. Syst.*, vol. 14, no. 1, pp. 37–47, 1997.
[7] D. R. Madill, D. W. L. Wang, and M. C. Ching, "A nonlinear observer for minimizing quantization effects in virtual walls," *Proc. ASME Dyn. Syst. Control Div.*, vol. 67, pp. 335–343, 1999.
[8] M. Goldfarb and J. Wang, "Passive stiffness simulation with rate-independent hysteresis," *Proc. ASME Dyn. Syst. Control Div.*, vol. 67, pp. 345–350, 1999.
[9] R. J. Adams and B. Hannaford, "Stable haptic interaction with virtual environments," *IEEE Trans. Robot. Autom.*, vol. 15, no. 3, pp. 465–474, Jun. 1999.
[10] B. Hannaford and J.-H. Ryu, "Time-domain passivity control of haptic interfaces," *IEEE Trans. Robot. Autom.*, vol. 18, no. 1, pp. 1–10, Feb. 2002.
[11] J.-H. Ryu, Y. S. Kim, and B. Hannaford, "Sampled and continuous time passivity and stability of virtual environments," in *Proc. IEEE Int. Conf. Robot. Autom.*, 2003, pp. 822–827.
[12] J.-H. Ryu, B. Hannaford, C. Preusche, and G. Hirzinger, "Time-domain passivity control with reference energy behavior," in *Proc. IEEE/RSJ Int. Conf. Intell. Robots Syst.*, 2003, pp. 2932–2937.
[13] S. Stramigioli, C. Secchi, A. J. van der Schaft, and C. Fantuzzi, "A novel theory for sample data system passivity," in *Proc. IEEE/RSJ Int. Conf. Intell. Robots Syst.*, 2002, pp. 1936–1941.
[14] B. E. Miller, J. E. Colgate, and R. A. Freeman, "On the role of dissipation in haptic systems," *IEEE Trans. Robot.*, vol. 20, no. 4, pp. 768–771, Aug. 2004.
[15] M. Mahvash and V. Hayward, "High-fidelity passive force-reflecting virtual environments," *IEEE Trans. Robot.*, vol. 21, no. 1, pp. 38–46, Feb. 2005.
[16] F. Janabi-Sharifi, V. Hayward, and C.-S. J. Chen, "Discrete-time adaptive windowing for velocity estimation," *IEEE Trans. Control Syst. Technol.*, vol. 8, no. 6, pp. 1003–1009, Nov. 2000.
[17] A. van der Schaft, L_2-*Gain and Passivity Techniques in Nonlinear Control*. London, U.K.: Springer-Verlag, 2000.
[18] N. Hogan, "Controlling impedance at the man/machine interface," in *Proc. IEEE Int. Conf. Robot. Autom.*, 1989, pp. 1626–1631.
[19] B. Armstrong-Helvouvry, P. DuPont, and C. C. de Wit, "Survey of models, analysis tools and compensation methods for the control of machines with friction," *Automatica*, vol. 30, no. 7, pp. 1083–1138, 1994.
[20] R. S. Strichartz, *The Way of Analysis*. Boston: Jones & Bartlett, 2000.
[21] J. J. Abbott and A. M. Okamura, "A sufficient condition for virtual wall passivity with quantization effects," in *Proc. ASME Dyn. Syst. Control Div.: Int. Mech. Eng. Congr. Expo.*, 2004, pp. 1065–1073.
[22] S. E. Salcudean and T. D. Vlaar, "On the emulation of stiff walls and static friction with a magnetically levitated input/output device," *ASME J. Dyn. Syst., Meas., Control*, vol. 119, pp. 127–132, 1997.
[23] J. D. Hwang, M. D. Williams, and G. Niemeyer, "Toward event-based haptics: Rendering contact using open-loop force pulses," in *Proc. 12th Symp. Haptic Interfaces Virtual Environ. Teleoperator Syst.*, 2004, pp. 24–31.
[24] A. M. Okamura, C. Richard, and M. R. Cutkosky, "Feeling is believing: Using a force-feedback joystick to teach dynamic systems," *ASEE J. Eng. Educ.*, vol. 92, no. 3, pp. 345–349, 2002.
[25] G. Strang, *Linear Algebra and Its Applications*, 3rd ed. Fort Worth, TX: Harcourt Brace Jovanovich, 1988.
[26] R. Horn and C. R. Johnson, *Matrix Analysis*. Cambridge, U.K.: Cambridge Univ. Press, 1985.
[27] S. W. Smith, *The Scientist and Engineer's Guide to Digital Signal Processing*. San Diego, CA: California Tech. Pub., 1997.
[28] D. G. Kleinbaum, L. L. Kupper, K. E. Muller, and A. Nizam, *Applied Regression Analysis and Other Multivariable Methods*, 3rd ed. Pacific Cove, CA: Duxbury Press, 1998.
[29] F. Al-Bender, V. Lampaert, and J. Swevers, "A novel generic model at asperity level for dry friction force dynamics," *Tribology Lett.*, vol. 16, no. 1–2, pp. 81–93, 2004.

Jake J. Abbott received the B.S. degree from Utah State University, Logan, in 1999, and the M.S. degree from the University of Utah, Salt Lake City, in 2001, both in mechanical engineering. He is currently working toward the Ph.D. degree in mechanical engineering at The Johns Hopkins University, Baltimore, MD.

His research interests include teleoperated and cooperative human–machine systems.

Allison M. Okamura (S'98–A'00) received the B.S. degree from the University of California, Berkeley, in 1994, and the M.S. and Ph.D. degrees from Stanford University, Stanford, CA, in 1996 and 2000, respectively, all in mechanical engineering.

She is an Assistant Professor of Mechanical Engineering with The Johns Hopkins University, Baltimore, MD. Her research interests include haptic display in virtual environments and teleoperation systems, medical robotics, and exploration with robotic fingers.